JOURNAL OF CATALYSIS 54, 318–335 (1978)

Reactions of Neopentane and Neohexane on Platinum/Y-Zeolite and Platinum/Silica Catalysts

K. FOGER AND J. R. ANDERSON[1]

CSIRO Division of Materials Science, Catalysis and Surface Science Laboratory, University of Melbourne, Parkville, Victoria, 3052, Australia

Received December 21, 1977; revised May 21, 1978

Isomerization and hydrogenolysis reactions of neopentane and neohexane have been studied in the presence of excess hydrogen at 455 to 625 K in a flow reactor over various Pt/silica and Pt/Y-zeolite catalysts having $\bar{d}_{Pt}$ in the range 1 to 20 nm. Additional catalyst characterization was provided by ESCA and by hydrogen TPD. Evidence is given to show that the reaction of neopentane was entirely confined to the platinum, even with Y-zeolite carrier. However, over Pt/Y-zeolite neohexane showed features which indicate dual-function catalytic behavior. As $\bar{d}_{Pt}$ decreased there was a general trend for the isomerization selectivity for neopentane (S_I) to decrease and for the activation energy (E_a) to increase. From the way in which S_I and E_a varied with $\bar{d}_{Pt}$, it is concluded that there are two reaction pathways for neopentane, one on low index crystallite facets, and a second at platinum atoms of low coordination, the probable site for the latter being a single platinum atom. Hydrogen TPD revealed an increasing proportion of higher energy binding sites at very small values of $\bar{d}_{Pt}$, and a correlation exists between S_I and the concentration of adsorbed hydrogen under reaction conditions as estimated by TPD. ESCA examination of Pt/Y-zeolite ($\bar{d}_{Pt} \approx 1$ nm) showed the presence of relatively electron-deficient platinum, the extent of this being greater for Pt/(La)Y- than for Pt/(Na)Y-zeolite. For the neopentane reaction, S_I and E_a were somewhat greater for Pt/(Na)Y- than for Pt/(La)Y-zeolite. Kinetic pressure dependence data showed that provided p_{H_2} was high enough, hydrogen was an inhibiting gas. Relative to the strength of hydrogen adsorption, the surface reaction intermediate from neopentane was adsorbed more strongly on Pt/silica ($\bar{d}_{Pt} \approx 4$ nm) than on Pt/Y-zeolite ($\bar{d}_{Pt} \approx 1$ nm). The nature of the adsorbed intermediates and the reaction pathways are discussed.

INTRODUCTION

Dispersed platinum catalysts offer two important experimental variables in skeletal hydrocarbon reactions. First, there is evidence for a platinum particle size effect with the hexanes, methylcyclopentane, and neopentane (*1–3*). Although dispersed platinum catalysts may provide dual-function catalytic behavior when the support offers a sufficiently effective acidic function, it is known that this platinum size effect can be observed when only the platinum is catalytically active (i.e., absence of dual-function activity): The conditions for this to be so are the use of supports of low acidity at 600 K or so and/or the use of neopentane as a model reactant for which a carbonium ion reaction pathway is improbable.

Second, there is evidence that varying the acidic strength of the support can affect the activity of supported platinum catalysts. There are two ways in which this may occur. When the catalyst is operating

[1] To whom all correspondence should be addressed.

0021-9517/78/0543-0318$02.00/0

under dual-function conditions, a change in the support acidity can be directly operative in its own right (e.g., *4*). Alternatively, as in the case of ethylene hydrogenation (*5*) and benzene hydrogenation (*7*) (reactions not involving skeletal rearrangements), where the reaction is thought to be entirely confined to the platinum, the catalyst activity is a function of the acidic strength of the support, probably due to changes in the electron concentration in those very small platinum particles which reside in the vicinity of electron-withdrawing (Lewis acid) sites.

Neopentane is an archetypal hydrocarbon reactant for platinum-only–catalyzed skeletal rearrangements. However, previous work with neopentane has been inadequate in two respects. The effect of varying support acidity has not been explored, although from the theory of the mechanism of the neopentane reaction (*8*) it should be favored by electron-deficient platinum. Furthermore, the relation between platinum particle size effects and kinetic parameters has not been examined thoroughly.

We have approached the problem in the following way. We have used neopentane as a molecule the reactions of which are entirely confined to the platinum: The use of suitable catalyst mixtures has confirmed this assumption. Neopentane thus allows an examination of the platinum function in a range of platinum/Y-zeolite catalysts in which the cation is varied, and in which it is possible to work with $\bar{d}_{Pt} < 2$ nm. Data have also been obtained using platinum/silica catalysts of varying dispersion. For comparison, we have examined the behavior of neohexane where a carbonium ion component to the reaction is to be expected in the presence of an acidic catalytic function. Since we are interested, *inter alia*, in changes to the electronic properties of highly dispersed platinum, we have examined our catalysts by ESCA. Furthermore, adsorbed hydrogen is a reactant in skeletal reactions of hydrocarbons and we have thus examined some of the catalysts by temperature-programmed desorption of hydrogen.

EXPERIMENTAL

Reactions were carried out using a flow reactor, generally operating in the differential mode at low conversions. The quantity of catalyst was in the region 0.2 to 0.4 g. Gas flow rates were in the range 0.2 to 3 cm^3 sec^{-1} with the contact time (t_c = catalyst free volume/flow rate) in the range of 0.18 to 1.8 sec.

To carry out a catalytic reaction, the catalyst was first reduced in a hydrogen flow (1 atm) overnight at 623 K; the reactor was then adjusted to the required reaction temperature, and the hydrogen flow was then replaced by the reactant flow.

The normal reaction mixture contained hydrogen and hydrocarbon in the molar ration of 20/1, and the reaction was carried out at 1 atm pressure. Thus, the normal reactant pressures were p_{H_2} = 96.50 kPa and p_{HC} = 4.83 kPa.

In some experiments the reactant partial pressures were varied in order to examine the kinetic pressure dependence of the reaction rate. This was done either by changing p_{H_2} and p_{HC} together so that $p_{H_2} + p_{HC} = 1$ atm or by diluting the hydrogen feed stream with argon while maintaining p_{HC} constant. In either case, these comparisons were made at constant total reactant stream flow rate.

The reactor effluent was analyzed by gas chromatography using a 65-m capillary column coated with HHK (Perkin–Elmer).

It is estimated that individual reaction rate values are known with a precision of $\pm 7\%$, and activation energies (obtained by least-squares fitting of the Arrhenius plots) are known to a precision of $\pm 5\%$.

Platinum/silica (Aerosil) catalysts were prepared in two ways. One series of catalysts was prepared by impregnation of Aerosil (Degussa 200; 200 m^2 g^{-1}) with

chloroplatinic acid solution using the method of incipient wetness, followed by air-drying at 400 K, and reduction in flowing hydrogen at 620 K. The catalyst composition was 0.9 wt% platinum (dry weight basis). Hydrogen adsorption measurement and electron microscopy gave a value for $\bar{d}_{Pt} = 4.0 \pm 0.2$ nm. Two other catalysts of increased $\bar{d}_{Pt}$ were prepared from this specimen by calcining in air or oxygen: 20 hr at 773 K in oxygen gave $\bar{d}_{Pt} = 7.0 \pm 0.5$ nm, and 24 hr at 1023 K in air gave $\bar{d}_{Pt} = 20.0 \pm 2$ nm, both these $\bar{d}_{Pt}$ values being obtained after subsequent hydrogen reduction. Another platinum/silica catalyst was prepared by adsorption of $Pt(NH_3)_4^{2+}$ from aqueous solution onto air-dried (400 K) Aerosil to give 1.95 wt% platinum (dry weight basis). After adsorption the sample was washed, dried at 400 K in air overnight, calcined in flowing oxygen at 573 K for 5 hr, and then reduced in flowing hydrogen at 623 K. Hydrogen adsorption measurement gave $\bar{d}_{Pt} = 1.1 \pm 0.1$ nm, while electron microscopy gave $\bar{d}_{Pt} = 1.3 \pm 0.5$ nm. For this sample we assign a mean value of $\bar{d}_{Pt} = 1.2$ nm.

Three platinum/Y-zeolite catalysts were prepared in which the exchangeable cations were Na^+, Ca^{2+}, La^{3+}, designated platinum/(Na)Y-zeolite, etc. All contained 3.0 wt% platinum. Platinum/(Ca)Y-zeolite was first prepared following the procedure of Dalla Betta and Boudart (*5*). The starting material, (Na)Y-zeolite (Linde SK-40), was converted into (Ca)Y-zeolite by exhaustive exchange with $Ca(NO_3)_2$ solution at 353 K, and into this $Pt(NH_3)_4^{2+}$ was then exchanged at 353 K to the extent of 3.0 wt% platinum (dry weight basis). After washing, the product was air-dried at 400 K overnight, calcined in flowing oxygen at 573 K for 5 hr, and then reduced in flowing hydrogen at 623 K for 16 hr. Samples of platinum/(Na)Y-zeolite and platinum/(La)Y-zeolite were prepared from the platinum/(Ca)Y-zeolite (after the generation of metallic platinum) by exhaustive exchange with solutions of $NaNO_3$ or $La(NO_3)_3$ at 353 K. Separate experiments showed that after the deposition of the metallic platinum, the remaining cations could be reversibly exchanged among the Na^+, Ca^{2+}, and La^{3+} states without loss of exchange capacity and without loss of platinum. This preparative procedure was adopted in order to ensure that the metallic platinum particles were located in the same position in the zeolite irrespective of the nature of the associated cation. All these platinum/Y-zeolite samples gave $\bar{d}_{Pt} = 1.0 \pm 0.1$ nm by hydrogen adsorption, while electron microscopy gave 1.0 ± 0.5 nm.

Hydrogen adsorption measurements were made using a static volumetric apparatus. Monolayer uptake was estimated from the linear portion of the room temperature isotherm at 1 to 7 kPa, and $\bar{d}_{Pt}$ was estimated on a spherical equivalent particle model after applying a blank correction for adsorption on the support (negligible in the case of Aerosil), and assuming a monolayer chemisorption stoichiometry of one hydrogen atom per surface platinum atom.

Electron microscopy was carried out using a Philips EM200, specimens being prepared by deposition of finely ground catalyst slurry onto a carbon-coated grid.

Catalyst compositions were obtained by XRF analysis.

The apparatus and procedure used for temperature-programmed desorption (TPD) of hydrogen followed, in the main, the description given by Aben *et al.* (*6*), and was based on a Carle Model 111H gas chromatograph.

ESCA measurements were made using an AEI spectrometer. Specimens were prepared from reduced platinum/Y-zeolite using inert atmosphere manipulation. After introduction into the spectrometer, the silicon 2*s* line was used as an internal energy standard, being set to 155.0 eV. Following the procedure of Scharpen (*9*), we confined our measurements to the $4f^{7/2}$–$4f^{5/2}$ doublet, thus giving the best results in terms of adequate sensitivity and sufficiently narrow linewidth. Nevertheless,

the aluminum $2p$ line overlaps platinum $4f^{5/2}$, and correction has to be made for this. We made this correction as follows. From measurements on platinum-free Y-zeolite we obtained data for the aluminum $2p$ and aluminum $2s$ lines. Noting that aluminum $2s$ does not overlap a platinum line, we used the aluminum $2s$ line from platinum/Y-zeolite to evaluate the aluminum $2p$ contribution to the spectrum from that sample, and by subtraction obtained the platinum-only spectrum. Full experimental details for the application of ESCA to supported platinum catalysts are given elsewhere (*24*).

RESULTS

Reaction products are expressed as the percentage of parent hydrocarbon converted to the specified product.

Reaction rates for the parent hydrocarbon are given either in units of molec sec^{-1} (g catalyst)$^{-1}$ (R_g), or molec sec^{-1} (m^2 Pt)$^{-1}$ (R_m), the use of the latter being confined to cases where the platinum is the sole seat of catalytic activity (neopentane). R_g and R_m were calculated from the percentage conversion, P, of parent hydrocarbon by

$$R_g = \frac{2.51 \times 10^{17} \times P \times f \times X_{HC}}{W_c}, \quad (1)$$

$$R_m = \frac{2.51 \times 10^{19} \times P \times f \times X_{HC}}{W_c \times X_{Pt} \times S_{Pt}}, \quad (2)$$

where f is the total reactant stream flow rate (cm^3 sec^{-1}) measured at room temperature (293 K), X_{HC} is the mole fraction of reactant hydrocarbon in the feed, W_c is the mass (g) of catalyst in the reactor, X_{Pt} is the weight percent of platinum in the catalyst, and S_{Pt} is the specific surface area of platinum in the catalyst [m^2 (g Pt)$^{-1}$]. S_{Pt} is related to the average platinum particle diameter, $\bar{d}_{Pt}$, by

$$S_{Pt} = 2.80 \times 10^2/\bar{d}_{Pt}, \quad (3)$$

where $\bar{d}_{Pt}$ is given in nanometers.

Product distributions are given at low conversion, in all cases $<10\%$ and in most cases $<1\%$, and at low contact times, ensuring negligible contribution from secondary reactions.

There are two reasons for believing that the measured reaction rates are uninfluenced by diffusional effects. First, varying the reactant flow rate over a range spanning more than one order of magnitude had no effect on the fractional conversion. Second, applying the diffusion criterion of Weisz and Praeter (*23*) gives a calculated effective diffusion parameter that is too small, by about two orders of magnitude compared with gaseous diffusion coefficients, for diffusional limitations to occur.

Reactions of Neopentane

Product distribution data are given in Table 1. Arrhenius plots for the variation of reaction rate with temperature are given in Fig. 1 while the corresponding activation energy data are included in Table 1.

In addition to reactions over the platinum catalysts, we also examined the reaction of neopentane over platinum-free (Na)Y- and (La)Y-zeolite catalysts: Product distributions are included in Table 1. These reactions were extremely slow compared to reactions over the platinum/zeolite catalysts. Thus, over platinum-free zeolite the reaction required a temperature of 623 K in order to reach the same rate as was achieved at 473 K over the corresponding platinum-containing catalyst. It is clear that, at the temperatures used with the platinum catalysts, the intrinsic activity of the platinum-free zeolites is negligible.

As a further check on possible dual-function catalytic conversion of neopentane, we have examined the product distributions obtained from its reaction over catalysts prepared as a physical mixture of platinum-containing component and platinum-free zeolite, so that these may be compared with the product distributions

TABLE 1

Data for Neopentane Reaction

Catalyst	Platinum dispersion (D) and average particle diameter ($\bar{d}_{Pt}$, nm)	Reaction temperature (K)	Reaction products[a] (%[b])						Isomerization selectivity[c]	Activation energy (kJ mol^{-1})
			M + E	P	i − B	n − B	i − P	n − P		
Pt/(Na)Y-zeolite; 3.0 wt% Pt	D = 1.05; $\bar{d}_{Pt}$ = 1.0	473	19.5	2.3	67.5	—	10.7	—	10.7	154
		513	21.5	4.6	65.3	—	8.6	—	8.6	
Pt/(Ca)Y-zeolite; 3.0 wt% Pt	D = 1.05; $\bar{d}_{Pt}$ = 1.0	473	23.3	3.4	69.2	—	4.1	—	4.1	146
		513	28.1	15.6	54.5	—	1.8	—	1.8	
Pt/(La)Y-zeolite; 3.0 wt% Pt	D = 1.05; $\bar{d}_{Pt}$ = 1.0	473	23.0	6.7	70.2	—	—	—	—	134
		513	31.6	23.2	45.2	—	—	—	—	
Pt/aerosil; 1.95 wt% Pt	D = 1.00; $\bar{d}_{Pt}$ = 1.2	533	16.6	5.4	30.3	3.5	43.2	1.0	44.2	146
		573	18.3	6.3	32.5	6.7	35.5	0.7	36.2	
Pt/aerosil; 0.9 wt% Pt	D = 0.28; $\bar{d}_{Pt}$ = 4.0	553	12.1	3.7	29.5	4.3	50.4	—	50.4	116
		593	16.6	4.4	29.6	4.6	42.0	2.8	44.8	
Pt/aerosil; 0.9 wt% Pt	D = 0.16; $\bar{d}_{Pt}$ = 7.0	553	8.2	4.5	23.6	2.8	60.9	—	60.9	104
		593	15.0	7.2	24.4	5.3	46.5	1.6	48.1	
Pt/aerosil; 0.9 wt% Pt	D = 0.057; $\bar{d}_{Pt}$ = 20.0	573	7.1	2.4	17.7	2.6	69.6	0.6	70.2	—
		613	14.1	6.2	20.2	—	52.0	7.5	59.5	
(Na)Y-zeolite (Pt-free)	—	623	26.5	8.6	36.1	—	28.8	—	28.8	—
(La)Y-zeolite (Pt-free)	—	623	28.1	11.5	37.0	—	23.4	—	23.4	—
Pt/(Na)Y-zeolite (3.0 wt% Pt) plus (La)Y-zeolite	D = 1.05; $\bar{d}_{Pt}$ = 1.0	523	19.3	2.2	66.5	—	12.0	—	12.0	—
Pt/aerosil (1.0 wt% Pt) plus (Na)Y-zeolite	e.m. $\bar{d}_{Pt} \approx 7$	623	16.2	7.3	18.4	—	56.0	2.1	58.1	
Pt/aerosil (1.0 wt% Pt) plus (La)Y-zeolite	e.m. $\bar{d}_{Pt} \approx 7$	623	14.2	6.9	14.7	—	58.0	6.2	64.2	—

[a] Primary products at low conversions (0.5–4%): M, methane; E, ethane; P, propane; i − B, isobutane; n − B, n-butane; i − P, isopentane; n − P, n-pentane.

[b] Expressed as percentage of parent converted to indicated product.

[c] Percentage of parent reacting to C_5 products.

obtained from zeolite-free platinum catalysts and from platinum-free zeolite. These mixtures were prepared by thorough grinding and mixing of the components in air, followed by processing according to the standard routine. The following mixtures were examined: [Pt/(Na)Y-zeolite] + [(La)Y-zeolite], 25/75 by weight; (Pt/Aerosil) + [(Na)Y-zeolite], 20/80 by weight; (Pt/Aerosil) + [(La)Y-zeolite], 20/80 by weight. Further details of the platinum-containing component are given in Table 1, which also gives the product distributions.

The dependence of the neopentane reaction on p_{H_2} and p_{HC} was examined over three catalysts: platinum/Aerosil (0.9 wt% Pt, $D = 0.28$, $\bar{d}_{Pt} = 4.0$ nm) at 573 to 577 K, platinum/(La)Y-zeolite and platinum/(Na)Y-zeolite (3.0 wt% Pt, $D = 1.05$, $\bar{d}_{Pt} = 1.0$ nm) at 493 to 501 K. The results are contained in Figs. 3 and 4. In addition, observations were made on the effect of reactant compositions on reaction selectivity over platinum/Aerosil ($\bar{d}_{Pt} = 4.0$ nm): (a) changing p_{H_2} from 18 to 101 kPa with p_{HC} at 1.73 kPa at 573 K resulted in the isomerization selectivity decreasing from 56.4 to 46.2%; (b) changing p_{HC} from 1.29 to 11.6 kPa with p_{H_2} at 101.3 kPa at 573 K resulted in the isomerization selectivity increasing from 44.7 to 65.0%; (c)

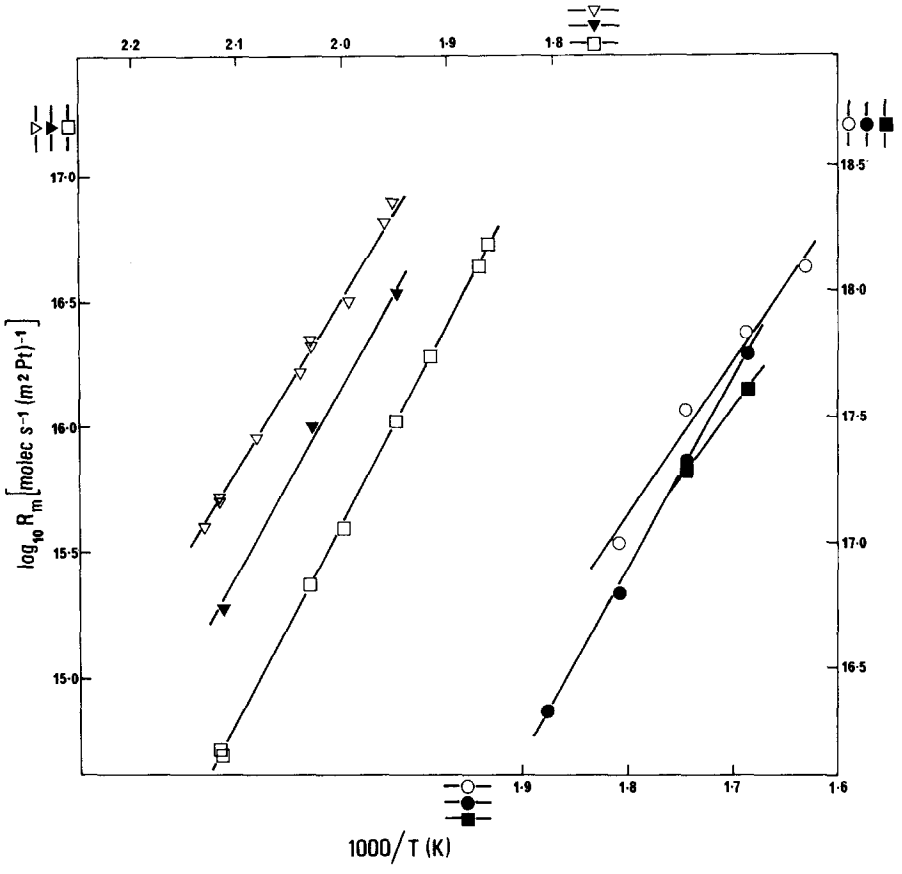

FIG. 1. Arrhenius plots for reaction of neopentane. ○, platinum/Aerosil (0.9 wt%, $\bar{d}_{Pt} = 4.0$ nm); ●, platinum/Aerosil (1.95 wt%, $\bar{d}_{Pt} = 1.2$ nm); ■, platinum/Aerosil (0.9 wt%, $\bar{d}_{Pt} = 7.0$ nm); ▽, platinum/(La)Y-zeolite (3.0 wt%, $\bar{d}_{Pt} = 1.0$ nm); ▼, platinum/(Ca)Y-zeolite (3.0 wt%, $\bar{d}_{Pt} = 1.0$ nm); □, platinum/(Na)Y-zeolite (3.0 wt%, $\bar{d}_{Pt} = 1.0$ nm).

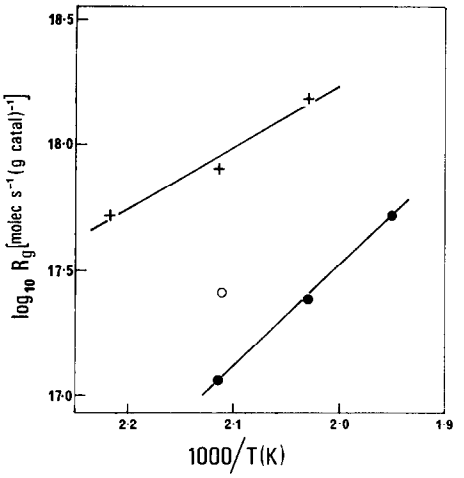

FIG. 2. Arrhenius plots for reaction of neohexane. +, platinum/(La)Y-zeolite (3.0 wt%, $\bar{d}_{Pt}$ = 1.0 nm); ●, platinum/(Na)Y-zeolite (3.0 wt%, $\bar{d}_{Pt}$ = 1.0 nm); ○, platinum/(Ca)Y-zeolite (3.0 wt%, $\bar{d}_{Pt}$ = 1.0 nm).

changing p_{HC} from 1.73 to 6.00 kPa with p_{H_2} at 40.0 kPa at 577 K resulted in the isomerization selectivity increasing from 56.0 to 62.1%. Over platinum/(La)Y-zeolite at 493 K, changing p_{H_2} from 101 to 10.1 kPa with p_{HC} constant at 1.01 kPa, resulted in only a slight change in the isomerization selectivity which increased from close to zero to about 0.5%.

Where comparison is possible, the reaction rates reported here are in satisfactory agreement with those obtained by other workers. Thus, at 545 K Dalla Betta and Boudart (*5*) reported a turnover number of 1.74×10^{-2} sec^{-1} for the total reaction over platinum/(Ca)Y-zeolite; after a short extrapolation to this temperature our figure is 1.89×10^{-2} sec^{-1}. At 573 K Leclercq *et al.* (*14*) reported a turnover number for the total reaction of 0.7×10^{-2} sec^{-1} over a 2 wt% platinum/alumina catalyst ($\bar{d}_{Pt} \approx 1.8$ nm); this may be compared with our figure of 1.7×10^{-2} sec^{-1} over a 1.95 wt% platinum/Aerosil catalyst ($\bar{d}_{Pt} \approx 1.2$ nm). Leclercq *et al.* (*14*) reported an activation energy of 168 kJ mol^{-1}, and this may be compared with our activation energies which lie in the range 134 to 156 kJ mol^{-1} for our various catalysts with $\bar{d}_{Pt}$ in the range 1.0 to 1.2 nm. As noted previously (*1*), the activation energy obtained by Boudart *et al.* (*3*) over a platinum/carbon catalyst ($\bar{d}_{Pt} \approx 20$ nm) is comparatively very large (ca. 230 kJ mol^{-1}) and may indicate a catalyst surface in some way modified by the presence of superficial carbon.

Reactions of Neohexane

Product distribution data are given in Table 2. Arrhenius plots for the variation of reaction rate with temperature are given in Fig. 2, while the corresponding activation energy data are included in Table 2. These reactions of neohexane were confined to platinum/Y-zeolite catalysts and to catalysts prepared as mixtures, viz., [Pt/(Na)Y-zeolite] + [(La)Y-zeolite], 20/80 by weight; (Pt/Aerosil)+[(Na)Y-zeolite], 20/80 by weight; (Pt/Aerosil) + [(La)Y-zeolite], 20/80 by weight (cf. also Table 2 for details).

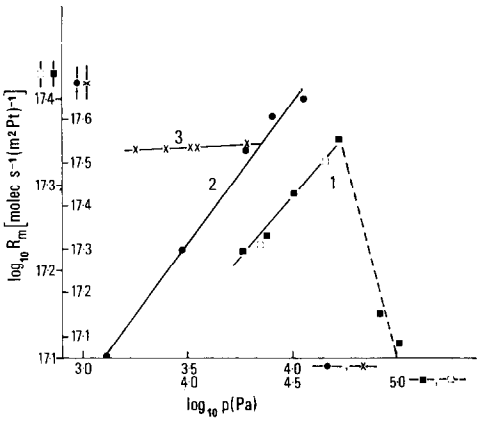

FIG. 3. Dependence of neopentane reaction rate, R_m, on reactant partial pressure. 1 (—■— and —□—, different experiments), variation of p_{H_2} with p_{HC} constant at 1.73 kPa. 2 (—●—), variation of p_{HC} with p_{H_2} constant at 101.3 kPa. 3 (—×—), variation of p_{HC} with p_{H_2} constant at 40.0 kPa. Reaction temperatures: 1 and 2, 573 K; 3, 577 K. Catalyst, platinum/Aerosil (0.9 wt% platinum, $\bar{d}_{Pt}$ = 4.0 nm).

ESCA Results

ESCA data for the platinum $4f^{5/2}$–$4f^{7/2}$ doublet from platinum/(Na)Y-zeolite and platinum/(La)Y-zeolite catalysts are contained in Fig. 5, after correction for the contribution from the aluminum $2p$ line. The error bars shown in Fig. 5 for the experimental profile are estimated from the counting statistics and from an estimate of the probable error resulting from the application of the aluminum $2p$ correction procedure.

The shapes of these experimental line profiles, particularly from platinum/(La)Y-zeolite, clearly indicate that there is more than a single platinum line contributing to each doublet component. Thus, for both samples each line component is considerably broader than that observed for a platinum reference, and in the case of platinum/(La)Y-zeolite the presence of an additional line is obvious from the presence of a shoulder at about 72.8 eV. We have effected a decomposition of each experimental profile into three contributing lines, using the following procedure.

We first noted that for a reduced platinum/Aerosil ($\bar{d}_{Pt}$ = 7.0 nm) catalyst the doublet lineshape (which was Gaussian) was closely similar to that observed for platinum foil. This basic doublet (e.g., curves 1 and 4 in Fig. 5) was thus used as the fundamental building unit in constructing a match to the experimental profile. A match required three contributing doublets, and these were adjusted in intensity (peak area) and energy, for best fit. The following constraints were imposed: In all cases the doublet components maintained the same (experimental) intensity ratio of 1/1.23 for the $4f^{5/2}$ and $4f^{7/2}$ components; the peak width (e.g., peak width at half-height) was constant at the value dictated by the platinum/Aerosil and platinum foil data; all line components were Gaussian; and the doublet separation was constant at the experimental value of 3.75 eV.

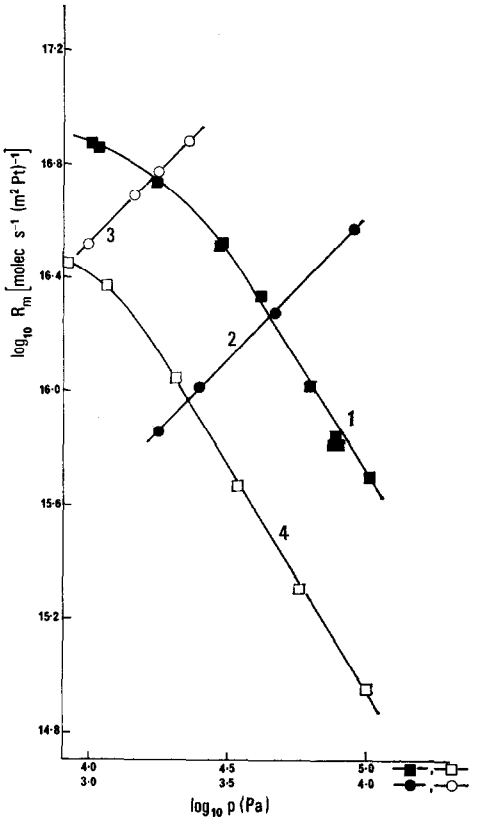

FIG. 4. Dependence of neopentane reaction rate, R_m, on reactant partial pressure. 1 (—■—), variation of p_{H_2} with p_{HC} constant at 1.01 kPa, at 495 K. 2 (—●—), variation of p_{HC} with p_{H_2} constant at 101.3 kPa, at 493 K. 3 (—○—), variation of p_{HC} with p_{H_2} constant at 26.6 kPa, at 493 K. 4 (—□—), variation of p_{H_2} with p_{HC} constant at 1.12 kPa, at 501 K. Catalyst, platinum/(La)Y-zeolite (3.0 wt% platinum, $\bar{d}_{Pt}$ = 1.0 nm), for curves 1, 2, 3; platinum/(Na)Y-zeolite (3.0 wt% platinum, $\bar{d}_{Pt}$ = 1.0 nm) for curve 4.

The resulting decomposition components are given in Fig. 5, from which it is seen that there is tolerable agreement between the experimental profile and that calculated by component summation; the only region where the computed profile lies appreciably outside the experimental error bars occurs at the high-energy tail of the platinum/(La)Y-zeolite profile. The relative component intensities and energies are listed in Table 3.

On both platinum/(Na)Y- and platinum/

TABLE 2

Data for Neohexane Reaction

Catalyst	Platinum dispersion (D) and average particle diameter (d_{Pt}, nm)	Reaction temperature (K)	Reaction products[a] (%[b])										Isomerization selectivity[c]	log (reaction rate)·(R_g molec sec^{-1} g cat^{-1})	Activation energy (kJ mol^{-1})
			M + E	P	i − B	n − B	i − P	n − P	2,3-DMB	2MP	3MP	n − H			
Pt/(Na)Y-zeolite, 3.0 wt% Pt	D = 1.05; d_{Pt} = 1.0	473	15.9	1.6	13.1	1.0	31.7	1.7	35.0	—	—	—	35.0	—[d]	76
		513	20.7	2.1	17.1	1.4	41.5	2.2	15.0	—	—	—	15.0		
Pt/(Ca)Y-zeolite, 3.0 wt% Pt	D = 1.05; d_{Pt} = 1.0	473	8.5	2.1	6.6	1.1	20.7	—	61.0	—	—	—	61.0	—[d]	—
Pt/(La)Y-zeolite, 3.0 wt% Pt	D = 1.05; d_{Pt} = 1.0	453	1.1	0.2	0.6	—	2.9	0.2	95.0	—	—	—	95.0	—[d]	48
		493	5.4	1.7	4.7	0.9	8.9	0.7	70.2	7.4		—	77.6		
Pt/(Na)Y-zeolite (3.0 wt% Pt) plus (La)Y-zeolite	D = 1.05; d_{Pt} = 1.0	523	6.6	2.2	4.6	—	14.4	1.3	69.0	1.9	—	—	70.9	17.62	—
Pt/aerosil (1.0 wt% Pt) plus (Na)Y-zeolite	e.m. $d_{Pt} \approx 7$	583	5.6	0.2	6.1	2.5	3.6	1.9	80.1	—	—	—	80.1	16.32	—
Pt/aerosil (1.0 wt% Pt) plus (La)Y-zeolite	e.m. $d_{Pt} \approx 7$	583	0.4	0.5	0.2	0.1	0.4	0.3	35.7	34.7	18.1	9.6	98.1	17.70	—

[a] Primary products at low conversions (<10%). M, methane; E, ethane; P, propane; i − B, isobutane; n − B, n-butane, i − P, isopentane; 2,3-DMB, 2,3-dimethylbutane; 2-MP, 2-methylpentane; 3-MP, 3-methylpentane; n − H, n-hexane.

[b] Cf. Table 1.

[c] Percentage of parent reacting to C_6 products.

[d] Cf. Figure 2.

(La)Y-zeolite, the higher-energy $4f^{7/2}$ components lie 1.2 and 2.4 eV above the Pt^0 line which is at 71.1 eV. For comparison, we note the shifts for the $4f^{7/2}$ line quoted by Escard *et al.* (*20*) of 2.0 to 2.6 eV for Pt^{2+} (2.6 eV for $PtCl_2$ and 2.0 eV for $Pt–O_{ads}$). Clearly our two components with $4f^{7/2}$ energies above Pt^0 correspond to species that are electron deficient compared to Pt^0. The small component with a shift of 2.4 eV may be reasonably indexed as Pt^{2+}, but the major component with a shift of 1.2 eV corresponds to a nominal valence between Pt^0 and Pt^{2+}, possibly Pt^+ as a formal assignment.

The data in Table 3 show that the electron-deficient platinum species are more abundant in platinum/(La)Y- than in platinum/(Na)Y-zeolite.

Temperature-Programmed Desorption Profiles

Four temperature-programmed desorption (TPD) profiles are recorded in Fig. 6

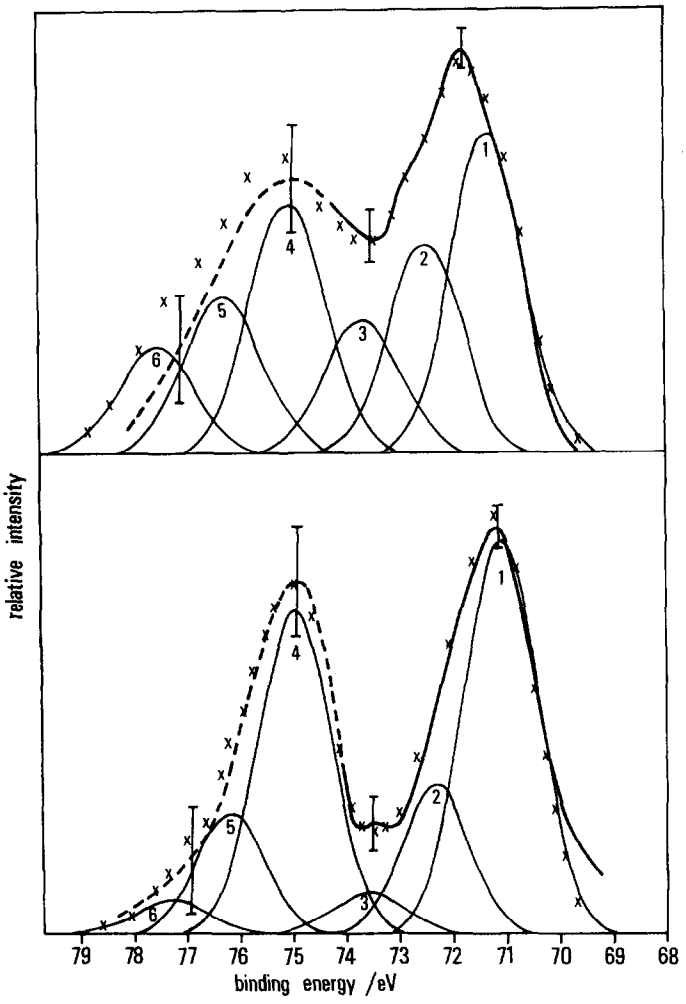

FIG. 5. ESCA data from platinum/(La)Y-zeolite (upper) and platinum/(Na)Y-zeolite (lower). Heavy line (full and broken) is the corrected experimental line profile; light lines are the fitted components; crosses give the component sums for comparison with the experimental profiles. The component numbering corresponds with that used in Table 3. For the fitting procedure see text.

TABLE 3

ESCA Component Data for Platinum/Y-Zeolite Catalysts

Catalyst	Component doublet[a]	Component relative intensity (%)	Component energy (eV)[b]
Pt/(La)Y	1,4	47	71.1
	2,5	32	72.3
	3,6	21	73.5
Pt/(Na)Y	1,4	69	71.1
	2,5	23	72.3
	3,6	8	73.5

[a] Identified in Fig. 5.

[b] For $4f^{7/2}$ part of doublet; for $4f^{5/2}$, add 3.75 eV.

for adsorbed hydrogen. Curves 1 and 2 were obtained from platinum/Aerosil, with $\bar{d}_{Pt}$ = 4.0 and 1.2 nm, respectively; curves 3 and 4 refer, respectively, to platinum/(La)Y- and platinum/(Na)Y-zeolite, both $\bar{d}_{Pt}$ = 1.0 nm. In all cases, the catalyst sample was reduced in a hydrogen flow at about 1 atm pressure and 630 K for about 16 hr. The sample was then cooled to room temperature in the hydrogen flow and equilibrated at room temperature for about 16 hr in a flow of sweep gas consisting of 0.1 vol% hydrogen in argon. Heating for TPD commenced at room temperature at a rate of 20 K min^{-1}.

In the case of the platinum/Aerosil catalysts, no correction was necessary for intrinsic adsorption on the support. However, with the platinum/Y-zeolite catalysts there is evidence for adsorption on the support both intrinsic and by a spillover process (*16*). The curves recorded in Fig. 6 for the platinum/Y-zeolite catalysts have been corrected for intrinsic adsorption on the zeolite, mainly by subtraction of a small peak having a maximum at about 750 K. Under the conditions used in the present work, we judge from previous evidence (*16*) that a spillover contribution will be negli-

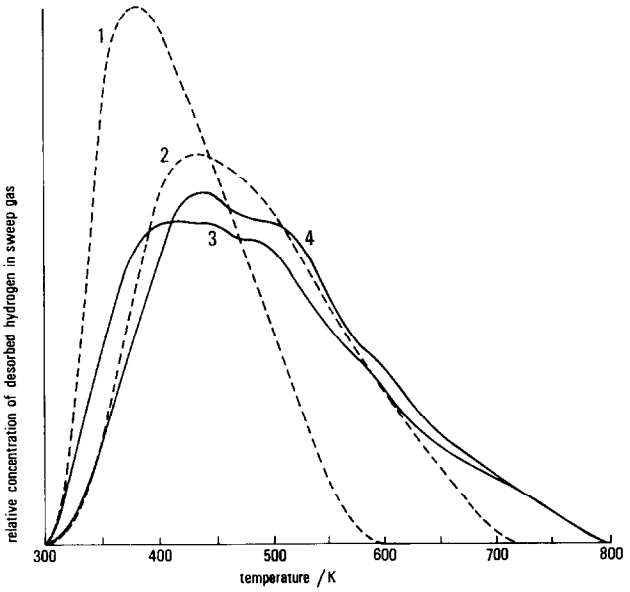

FIG. 6. Temperature desorption profiles. Curves (– – –) are for platinum/Aerosil catalysts, curves (——) are for platinum/Y-zeolite catalysts. 1, platinum/Aerosil, $\bar{d}_{Pt} \geqslant 4.0$ nm; 2, platinum/Aerosil, $\bar{d}_{Pt}$ = 1.2 nm; 3, platinum/(La)Y-zeolite, $\bar{d}_{Pt}$ = 1.0 nm; 4, platinum/(Na)Y-zeolite, $\bar{d}_{Pt}$ = 1.0 nm. The curves have been scaled to equal areas (equal amounts of adsorbed hydrogen). Heating rate, 20 K min^{-1}; sweep gas argon with 0.1 vol% H_2.

gible. However, there is a small residual uncertainty about this conclusion, and accordingly that part of the profile where, given appropriate conditions (*16*), spillover can become evident (>700 K), is regarded as being defined with less accuracy than the rest.

The TPD profiles are clearly dependent on platinum particle size for $\bar{d}_{Pt} < 4.0$ nm. Thus profiles 2, 3, and 4, which refer to $\bar{d}_{Pt}$ in the range 1.0 to 1.2 nm, all are much broader with more extensive high-temperature tails than is curve 1, which refers to $\bar{d}_{Pt} \geqslant 4.0$ nm. It is also seen that curves 2, 3, and 4 have maxima in the region 420 to 440 K compared with 385 K for curve 1. Furthermore, for platinum/Y-zeolite the main maximum is partly resolved into subsidiary maxima, and there is also a partly resolved shoulder at about 600 K, the presence of which has been noted previously (*16*).

Reasons are given elsewhere (*22*) for concluding that diffusional effects in the support are not of major importance in determining profile shape. The data in Fig. 6 confirm this, since profiles 2, 3, and 4 are fairly similar in shape while the supports are widely different. For the present purpose, the most important qualitative conclusion to be drawn from these TPD profiles is that platinum particles in the size range 1.0 to 1.2 nm offer a substantially greater proportion of higher-energy binding states for hydrogen than is available for $\bar{d}_{Pt} \geqslant 4.0$ nm.

DISCUSSION

The Effect of Platinum Particle Size

Figure 7 summarizes our data for the isomerization selectivity of the neopentane reaction, together with corresponding activation energy data. For comparison, we include in this figure some earlier data by Boudart *et al.* (*3*, *5*). Inasmuch as earlier results suggested that skeletal reactions of neopentane were favored on (111) platinum surfaces (*3*, *10*), we also include in Fig. 7

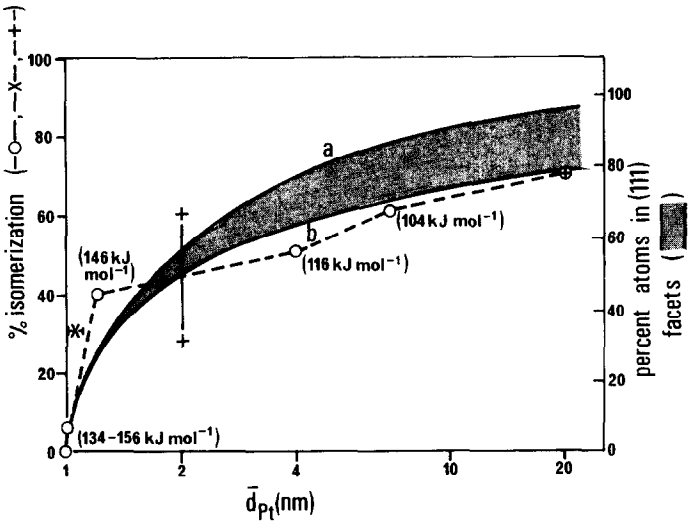

FIG. 7. Parameters for neopentane reaction as a function of average platinum particle size ($\bar{d}_{Pt}$). Parenthetic numerical values are for the overall activation energy. The band of values for the percentage of surface atoms in (111) facets is bounded by data for octahedral crystallites (a) and for cubo-octahedral crystallites (b). The two ordinate scales were normalized with respect to each other, as described in the text. –○–, this work; – + –, Boudart *et al.* (*3*). The range + – + is for catalysts with varying thermal histories at constant $\bar{d}_{Pt}$, a variation thought to induce variations in crystallite shape (*3*); the data |–×–| is for a platinum/(Ca)Y-zeolite catalyst with $D \approx 1$ (*5*).

data showing, as a function of platinum particle size (diameter of equivalent spherical particle), the relative proportion of surface atoms occurring in (111) facets. These data are given as a band limited by values for octahedral (upper bound) and cubo-octahedral (lower bound) crystalline shapes; all of the common high-symmetry crystallite shapes give data falling within this band. The scales for isomerization selectivity and proportion of surface atoms occurring in (111) facets were normalized one against the other by making use of the information that a 100% (111) surface is estimated to give an isomerization selectivity of 90% (based on corresponding data for isobutane, *10*).

The following are the main features to be seen from Fig. 7. There is a general trend for the neopentane isomerization selectivity to fall with decreasing $\bar{d}_{Pt}$ below about 20 nm, and most of this change occurs for particles below about 1.5 nm in size. This trend follows approximately the variation in the proportion of surface atoms in (111) facets, and this agreement is sufficient to support the hypothesis (*3*, *10*) that the proportion of surface atoms in (111) facets is an important factor in controlling the isomerization selectivity. In making this comparison, it should be remembered that the actual platinum particle shapes would be expected to be less regular than the assumed ideal shapes, and this would depress the experimental selectivity below that to be expected for ideal crystallites—a variation in the direction indicated by Fig. 7.

The result (also included in Fig. 7) due to Dalla Betta and Boudart (*5*) for the reaction of neopentane on a platinum/(Ca)Y-zeolite catalyst requires special comment. This catalyst had a dispersion quoted as unity (*5*) and was prepared in a temperature regime roughly similar to that used in the present work. Nevertheless, it gave an isomerization selectivity of 31% at about the same reaction conditions as used in the present work, and this needs to be compared to our own platinum/Y-zeolite catalysts, which gave isomerization selectivities $<10\%$. We believe that this difference is not an artifact, but has its origin in the following factors. In the platinum particle size range <1.5 nm, the reaction selectivity appears to vary very rapidly with size, but it is in this range where $\bar{d}_{Pt}$ is known with only very limited accuracy. Thus for platinum, $D = 1.0$ is consistent with $\bar{d}_{Pt} \leqslant 1.1$ nm, and it is possible that $\bar{d}_{Pt}$ for Boudart's catalyst was significantly greater than ours. Furthermore, although prepared by nominally the same method, one has no guarantee that both catalysts consisted of platinum particles of identical shape or size distribution since the preparative conditions (e.g., temperature/time regime) were not identical. The comparison serves to emphasize the difficulty of obtaining adequate control over the experimental variables in this range of $\bar{d}_{Pt}$.

There is a trend for the overall activation energy for the neopentane reaction to increase with decreasing $\bar{d}_{Pt}$. However, the activation energy varies with $\bar{d}_{Pt}$ in a rather different way to the isomerization selectivity at low values of $\bar{d}_{Pt}$ (<1.2 nm). In this region the isomerization selectivity varies strongly with $\bar{d}_{Pt}$, but the activation energy is relatively insensitive.

The fact that the activation energy for the neopentane reaction varies with $\bar{d}_{Pt}$ makes it clear that the nature of this reaction cannot be understood solely in terms of the surface geometry of the platinum catalyst—as would be implicit in a description couched only in terms of the proportion of surface atoms in (111) facets. The question immediately arises whether the reason for the variation in activation energy with $\bar{d}_{Pt}$ can be reasonably sought in the variation with $\bar{d}_{Pt}$ of the electronic properties of the platinum crystallites. For the following reasons we answer this question in the negative.

There is now considerable theoretical

evidence (*17–19*) that the electronic properties of a small metallic particle will only differ significantly from those of the bulk metal if the particle contains less than about a few tens of atoms. In other words, such a difference will only be manifested for particles with $\bar{d}_{Pt}$ less than about 1 nm. This picture is only consisted with our observed dependence of activation energy on $\bar{d}_{Pt}$ if it is assumed that the latter is not principally controlled by changes in the intrinsic electronic properties of the platinum.

We propose, therefore, that our results are a consequence of the operation of parallel pathways which have different activation energies, and the relative proportions of which are particle size dependent.

The model we have adopted is as follows.

Pathway 1. For this we propose the mechanism as originally formulated (*3*, *10*) and since well accepted (*1*), involving the adsorbed intermediates (A) and/or (B).

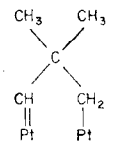

(A)

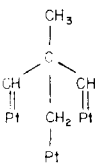

(B)

As suggested by Boudart (*3*), it is possible that (B) operates with some preference over (A) on (111) surfaces or facets of platinum, and favors isomerization to a greater extent than (A). However, it seems unlikely that this difference, if real, will be of dominant importance, because results with isobutane show (*10*) that on (100) platinum the isomerization selectivity is still about 70% of that on (111) platinum, despite the inability of an intermediate such as (B) to occur at all on (100) platinum.

Pathway 2. This reaction must occur at a platinum surface site which is relatively abundant for $\bar{d}_{Pt} \approx 1$ nm, but whose relative abundance falls rapidly as $\bar{d}_{Pt}$ increases. This pathway must also be capable of yielding a high selectivity to hydrogenolysis (cf. behavior of neopentane with Pt/Y-zeolite catalysts for $\bar{d}_{Pt} \approx 1$ nm), although as will be discussed later, the relative importance of hydrogenolysis vs isomerization also depends on the concentration of adsorbed hydrogen relative to hydrocarbon.

The requirement that pathway 2 may be strongly biased toward hydrogenolysis makes it clear that the differentiation between pathways 1 and 2 is not to be sought in terms of intermediates (A) and (B), since both of these are known to yield substantial isomerization activity. Furthermore, since (A) requires a pair of nearest-neighbor surface platinum atoms (*10*), it would be difficult to see how this requirement could be consistent with the rapid increase in the relative importance of pathway 2 at very small values of $\bar{d}_{Pt}$, unless the platinum atoms were in a step edge. While this possibility cannot be definitely ruled out, it seems more likely that pathways 1 and 2 involve basically different mechanisms.

We therefore design a model in which pathway 2 operates at a single surface platinum atom. We further propose that a low coordination platinum atom (corner or edge atom) is a favored reaction site since the surface concentration of such atoms increases rapidly in the range of $\bar{d}_{Pt}$ less than about 2 nm.

Mechanisms for the skeletal rearrangement of hydrocarbons by bond shift at a single platinum atom site have already been suggested by Sammon *et al.* (*11*, *12*) and by Gault *et al.* (*2*).

We consider Sammon's mechanism in more detail since it has some supporting evidence from steric considerations and from deuterium exchange results (*11*, *12*). When specialized for neopentane this mechanism may be represented as in expression (4), which differs from that pro-

posed (*11*, *12*) only in the recognition that hydrogenolysis may occur from the π-adsorbed intermediate (C) from attack by hydrogen:

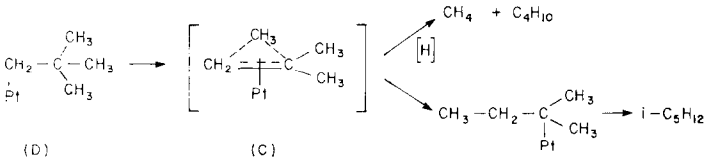

---- (4)

From the mechanism proposed for the neopentane reaction, one would expect the reaction selectivity to be sensitive to the concentration of hydrogen adsorbed on the catalyst surface under reaction conditions. We estimate the relative amounts of adsorbed hydrogen from the TPD profiles (cf. Fig. 6), by comparing the relative proportions of each profile occurring above the reaction temperature. Using the typical reaction temperatures of 560 and 480 K for the platinum/Aerosil and platinum/Y-zeolite catalysts, respectively, we estimate the proportions of the TPD profiles occurring above these temperatures, and the results are

platinum/Aerosil
($\bar{d}_{Pt}$ = 4.0 nm), >560 K, 1%;
platinum/Aerosil
($\bar{d}_{Pt}$ = 1.2 nm), >560 K, 18%;
platinum/(La)Y-zeolite
($\bar{d}_{Pt}$ = 1.0 nm), >480 K, 45%;
platinum/(Na)Y-zeolite
($\bar{d}_{Pt}$ = 1.0 nm), >480 K, 52%.

These data can only be used in a comparative sense because the hydrogen pressure under reaction conditions is considerably greater than that under which the hydrogen is adsorbed for TPD. Bearing this in mind, some qualitative correlations emerge.

Since the TPD profiles are essentially invariant for $\bar{d}_{Pt} > 4.0$ nm, the concentration of adsorbed hydrogen under reaction conditions is also invariant: Thus, in this size range the dependence of the reaction selectivity on $\bar{d}_{Pt}$ must be entirely a function of surface geometry (cf. the variation in the proportion of (111) facets). On the other hand, platinum/Aerosil $\bar{d}_{Pt}$ = 1.2 nm, which yielded 18% of the TPD profiles above the reaction temperature, gave about 60% of reaction by hydrogenolysis, whereas platinum/Y-zeolite $\bar{d}_{Pt}$ = 1.0 nm, which yielded 45 to 52% of the TPD profile above the reaction temperature, gave $\geqslant$90% of the reaction by hydrogenolysis. The similarity of the activation energies on these catalysts and the closeness of their $\bar{d}_{Pt}$ values points to the same basic reaction mechanism, that is to say, reaction (4) involving a single surface platinum atom, with an increased concentration of surface hydrogen on platinum/Y-zeolite diverting an increased proportion of reacting neopentane toward hydrogenolysis. This conclusion also involves the proposal that intermediate (C) in reaction (4) is diverted toward hydrogenolysis via attack by adsorbed hydrogen rather than gas phase hydrogen, and this is a conclusion which is substantiated by kinetic pressure dependence data (*vide infra*).

Kinetic Pressure Dependence

It will be noted from Figs. 3 and 4 that on platinum/Aerosil ($\bar{d}_{Pt}$ = 4.0 nm), the rate at 573 K passes through a maximum at about $p_{H_2} \approx 50$ kPa with p_{HC} = 1.73 kPa. This is in reasonably good agreement

with the results of Leclercq *et al.* (*14*) who observed a similar maximum at about 40 kPa with p_{HC} = 10.1 kPa at 586 K. Our data show that over platinum/Y-zeolite catalysts similar maxima are not found, although there is some evidence (cf. Fig. 4) for a trend toward the formation of maxima at the bottom end of the p_{H_2} range.

The data in Figs. 3 and 4 may be used to evaluate the exponents n and m in the pressure dependence expression,

$$\text{rate} \propto p_{HC}{}^n p_{H_2}{}^m. \qquad (5)$$

The results are collected into Table 4 where we refer to the rate of the total reaction. In the case of reactions on the platinum/Y-zeolite catalysts the total reaction was essentially confined to hydrogenolysis. With the platinum/Aerosil, both isomerization and hydrogenolysis were important, and kinetic pressure dependencies for both these reactions may be evaluated by using the kinetic data for the total reaction together with the variation of product distribution with changing reactant composition. The results (on platinum/Aerosil, $\bar{d}_{Pt}$ = 4.0 nm) are as follows: isomerization, $n \approx (x + 0.1)$, $m \approx (y - 0.1)$, hydrogenolysis, $n \approx (x - 0.1)$, $m \approx (y + 0.1)$; where x and y are the corresponding exponents for the total reaction listed in Table 4.

The pressure dependence data suggest the following conclusions. Relative to the strength of adsorption of hydrogen, the surface reaction intermediate from neopentane is adsorbed more strongly on platium/Aerosil, $\bar{d}_{Pt}$ = 4.0 nm, than on platium/Y-zeolite (cf. the larger value of n in $p_{HC}{}^n$ over platium/Y-zeolite than platium/Aerosil, and the shift in the position of the rate maximum to a lower value of p_{H_2} over platinum/Y-zeolite). This change in the relative strength of neopentane adsorption agrees qualitatively with the proposals made in the previous section for the nature of the adsorbed intermediates.

Provided p_{H_2} is high enough, hydrogen is an inhibiting gas. In view of the fact that (on platinum/Aerosil) the hydrogen pressure dependence exponent changes from −0.9 to 0.3 as p_{H_2} falls into the region 20 to 50 kPa, it is reasonable to conclude that at higher hydrogen pressures the catalyst surface is heavily covered with hydrogen. This is relevant to the difference in the value of m in the kinetic pressure dependence term $p_{H_2}{}^m$ for the hydrogenolysis and isomerization reactions ($\Delta m = m_{hydrog} - m_{ism} \approx 0.2$). When isomerization and hydrogenolysis occur from the same adsorbed intermediate (A or B), hydrogenolysis results when the intermediate is attacked by hydrogen (*10*). Thus, with Δm = 0.2, the attacking hydrogen cannot be gas phase molecular hydrogen for which one would find Δm = 1. We conclude that attack occurs by chemisorbed hydrogen for which, on a heavily covered surface, the surface concentration is proportional to a low power of the hydrogen pressure.

TABLE 4

Kinetic Pressure Dependence Exponents
Rate $\propto p_{HC}{}^n p_{H_2}{}^m$

Catalyst	Pressure dependence	Conditions
Platinum/Aerosil $\bar{d}_{Pt}$ = 4.0 nm 573–577 K	$p_{HC}{}^{0.7} p_{H_2}{}^{-0.9}$	p_{H_2}, 60–100 kPa p_{HC}, 1.3–12 kPa
	$p_{HC}{}^{0.04} p_{H_2}{}^{0.3}$	p_{H_2}, 20–50 kPa p_{HC}, 1.8–6 kPa
Platinum/(La)Y-zeolite $\bar{d}_{Pt}$ = 1.0 nm 493–495 K	$p_{HC}{}^{1.0} p_{H_2}{}^{-1.5}$	p_{H_2}, 27–100 kPa p_{HC}, 1.7–9 kPa

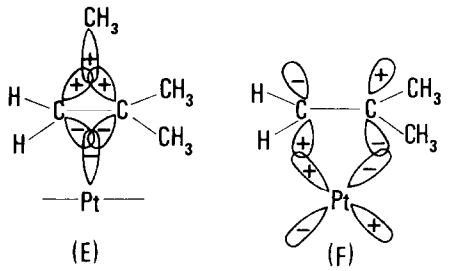

FIG. 8. Bonding scheme for surface intermediate (C) in reaction (4); cf. Samman *et al.* (*11*).

Reaction on Platinum/Y-zeolite Catalysts

Neopentane. In the reactions of neopentane on platinum/Y-zeolite catalysts, two main trends emerge. The activation energy for the total reaction (mainly hydrogenolysis) increases in the sequence 134, 146, 154 kJ mol^{-1} as the nature of the associated cation changes in the order La^{3+}, Ca^{2+}, Na^{+}, while at the same time isomerization selectivity at 473 K (for instance) changes in the sequence 0, 4.1, 10.7%. We reiterate the point made in an earlier section that the nature of the reactant molecule and the relatively very low catalytic activity of platinum-free zeolite for the neopentane reaction strongly support the contention that the reaction is entirely confined to the platinum.

Following the discussion in earlier sections, we propose to consider the neopentane reaction over these catalysts in terms of a single platinum atom reaction site, that is, in terms of reaction (4) in the present formulation.

ESCA data show that in our platinum/(La)Y-zeolite catalysts (with very small platinum particles, $\bar{d}_{Pt} \approx 1.0$ nm), the platinum behaves as though it were electron deficient compared to bulk metallic platinum. This agrees with conclusions reached from chemical evidence by previous workers (*5*, *15*). Furthermore, our data show that the platinum particles appear to be more electron deficient when the associated cation is La^{3+} rather than Na^{+}. We therefore seek a model which will correlate an increased electron deficiency of the platinum with a lower activation energy for the neopentane reaction.

We refer to the two molecular orbitals (cf. Fig. 8) by which the reaction intermediate (C) in reaction (4) is considered bonded to a surface platinum atom: This follows the proposals detailed by Samman *et al.* (*12*). Of these, orbital (F) of Fig. 8 is nonbonding to the labile methyl group, while (E) of Fig. 8 is bonding to that group. If, for instance, and as would seem very probable given the transient nature of (C), one of these (C) orbitals lies at an appreciably higher energy than the top filled orbital involved in bonding the precursor (D) to the surface (cf. reaction (4)), a partial depopulation of this uppermost (C) orbital would lower the energy of (C) relative to that of (D).

Samman *et al.* (*12*) have already pointed out that in forming orbital (F) the energy of the olefinic $p\pi^*$ orbital will be substantially lowered by overlap with the platinum $d\pi$ orbital so that the resultant molecular orbital is now of sufficiently low energy to be occupied. If in this way the energy of orbital (F) is lowered sufficiently to lie below that of orbital (E), it will be orbital (E), which is principally depopulated by an electron withdrawal process, and this would result in an enhanced reactivity of the labile methyl group. The change in isomerization selectivity on going from platinum/(La)Y- to platinum/(Na)Y-zeolite (zero vs 10.7% at 473 K) appears to be correlated with the increased methyl group reactivity.

It may be noted that there is evidence both from calculations (*13*) and from work-function measurement (*21*) that surface atoms of low coordination (e.g., corner atoms) are more electron deficient than atoms of higher coordination in a surface plane, and this difference is particularly great for platinum because of the high density of states at the Fermi level. This may perhaps be the reason why reaction (4)

occurs preferentially at low coordination platinum atom sites.

Neohexane. The isomerization selectivity varies strongly with the nature of the associated cation in the platinum/Y-zeolite catalysts, the selectivity at 473 K increasing in the sequence 35.0, 61.0, and 95.0% for the cations Na^+, Ca^{2+}, and La^{3+}, respectively. This behavior is consistent with the reaction of neohexane via a carbonium ion mechanism on a dual-function catalyst, the strength of the acidic function of which increases strongly in the order Na^+, Ca^{2+}, La^{3+}. This latter is in agreement with previous reports (*4*). The fact that the activation energy is greater on platinum/(Na)Y- than on platinum/(La)Y-zeolite (cf. Table 2) suggests that the rate-controlling step occurs on the acidic function, also in agreement with the accepted model for this type of reaction.

ACKNOWLEDGMENTS

The authors are grateful to Dr. J. V. Sanders for valuable help with electron microscopy, to Dr. F. Larkins of Monash University for taking the ESCA data, and to Mr. R. Sherwood for general experimental assistance.

REFERENCES

1. Anderson, J. R., *Advan. Catal.* **23**, 1 (1973).

2. Garin, F., and Gault, F. G., *J. Amer. Chem. Soc.* **97**, 4466 (1975); Dartiques, J-M., Chambellan, A., and Gault, F. G., *J. Amer. Chem. Soc.* **98**, 856 (1976).

3. Boudart, M., Aldag, A. W., Ptak, L. D., and Benson, J. E., *J. Catal.* 11, 35 (1968); Boudart, M., and Ptak, L. D., *J. Catal.* **16**, 90 (1970).

4. Pickert, P. E., Rabo, J. A., Dempsey, E., and Schomaker, V., *in* "Proceedings, 3rd International Congress on Catalysis" (W. M. H. Sachtler, G. C. A. Schuit, and P. Zwietering, Eds.), p. 714. North-Holland, Amsterdam, 1965.

5. Dalla Betta, R. A., and Boudart, M., *in* "Proceedings, 5th International Congress on Catalysis" (J. W. Hightower, Ed.), p. 1329. North-Holland, Amsterdam, 1973.

6. Aben, P. C., van der Eijk, and Oelderik, J. M., *in* "Proceedings, 5th International Congress on Catalysis" (J. W. Hightower, Ed.), p. 717. North-Holland, Amsterdam, 1973.

7. Figueras, F., Gomez, R., and Primet, M., "Molecular Sieves," Advances in Chemistry Sieves, Vol. 121, p. 480, 1973.

8. Anderson, J. R., and Avery, N. R., *J. Catal.* **7**, 315 (1967).

9. Scharpen, L. H., *J. Electron Spectrosc. Related Phenomena* **5**, 369 (1974).

10. Anderson, J. R., and Avery, N. R., *J. Catal.* **5**, 446 (1966).

11. Samman, N. G., *in* "Proceedings, 5th International Congress on Catalysis" (J. W. Hightower, Ed.), p. 711. North-Holland, Amsterdam, 1973.

12. McKervey, M. A., Rooney, J. J., and Samman, N. G., *J. Catal.* **30**, 330 (1973).

13. Tsang, Y. W., and Falicov, L. M., *J. Phys. C, Solid State Phys.* **9**, 51 (1976).

14. Leclercq, G., Leclercq, L., and Maurel, R., *J. Catal.* **44**, 68 (1976).

15. Gallezot, P., Datka, J., Massardier, J., Primet, M., and Imelik, B., *in* "Proceedings, 6th International Congress on Catalysis" (G. C. Bond, P. B. Wells, and F. C. Tompkins, Eds.), p. 696. The Chemical Society, London, 1977.

16. Anderson, J. R., and Breakspere, R. J., *in* "Proceedings, 7th International Vacuum Congress and 3rd International Conference on Solid Surfaces," Vol. 1, p. 823. 1977.

17. Anderson, J. R., "Structure of Metallic Catalysts." Academic Press, London, 1975.

18. Baetzold, R. C., *J. Phys. Chem.* **80**, 1504 (1976).

19. Primet, M., Basset, J. M., Garbowski, E., and Mathieu, M. V., *J. Amer. Chem. Soc.* **97**, 3655 (1975).

20. Escard, J., Pontvianne, B., Chenebaux, M. T., and Cosyns, J., *Bull. Soc. Chim. Fr.* 2399 (1975).

21. Besocke, K., Kral-Urban, B., and Wagner, H., *Surface Sci.* **68**, 39 (1977).

22. Anderson, J. R., Foger, K., and Breakspere, R. J., submitted for publication.

23. Weisz, P. B., and Praeter, C. D., *Advan. Catal.* **6**, 143 (1954).

24. Larkins, F. P., Hughes, M. E., Anderson, J. R., and Foger, K. *Australian Conference on Electron Spectroscopy, Proceedings. 1978.* Elsevier, Amsterdam.